IMPROVED SURFACE WAVE DETECTION AND MEASUREMENT USING PHASE-MATCHED FILTERING WITH A GLOBAL ONE-DEGREE DISPERSION MODEL

Jeffry L. Stevens, David A. Adams, and G. Eli Baker

Science Applications International Corporation

Sponsored by Defense Threat Reduction Agency

Contract No. DSWA01-98-C-0154

ABSTRACT

The primary goal of this project is to improve the capability to identify and detect surface waves for the purpose of earthquake/explosion discrimination. We are developing improved, higher resolution earth and dispersion models. The models consist of approximately 600 distinct crust and upper mantle structures, with surface layering and/or ocean depths that vary on a one-degree grid. There are a total of 64,800 earth models and dispersion curves, but the tomographic inversion is performed only for the 600 distinct crust and upper mantle models, with the shallow structure constrained by other information. The data set used in the inversion now consists of approximately 548,000 phase and group velocity dispersion measurements obtained from a variety of sources. Surface sediments are defined using the global sediment maps of Laske and Masters (1997), and ocean bathymetry is defined using the Etopo5 topographic data set.

Automatic identification of surface waves at the International Data Centre is currently performed by narrow-band filtering the data at several frequencies, and then comparing the arrival times with a regionalized dispersion model. We have implemented and tested a new procedure in which we first phase-match filter the data and then apply narrow-band filters to the compressed waveform and use a detection test similar to the current test. This allows us to take advantage of the improved signal-to-noise ratio of the phase-match filtered waveforms, while retaining the robustness of narrow-band filtering for frequency-dependent signal identification. After phase-matched filtering, the predicted arrival time is zero at all frequencies, so we test to see if the arrivals are within a time window similar to that used in the existing test. To test the procedure, we processed the same data set using five-degree and one-degree models with and without phase-matched filtering. Detections using the one-degree model with phase-matched filtering increased by more than 30% compared to the five-degree model currently in use at the IDC without phase-matched filtering.

We use long-period waveforms from historic nuclear explosions to assess the potential of automated Rayleigh wave travel-time picks to improve seismic event locations. The improved accuracy of locations reported by Yacoub (2000), based on 20-second Rayleigh waves, provided the impetus for this work. Although surface wave arrival times cannot be measured as accurately as body wave arrivals, that surface waves are much slower means that accurate locations can be achieved. We find that good locations can be determined with surface waves, which could potentially improve locations made with body waves alone provided that the paths are relatively short and an accurate dispersion model is available for the region. This may be especially important for small events with few total measurements. To assess the value of single surface wave measurements for that purpose, we also estimate the accuracy of single-station distance estimates.

KEY WORDS: surface wave, dispersion curve, phase-matched filter, regionalization, moment, location

OBJECTIVE

The primary objective of this project is to develop improved methods for detection and measurement of surface waves. This is important because the threshold level for surface waves is, in general, the threshold

for the M_s:m_b discriminant. By reducing the threshold for surface wave detection, we can reduce the number of unidentified events and increase the likelihood of identifying smaller nuclear explosions.

RESEARCH ACCOMPLISHED

As stated above, the primary focus of this project is to improve the capability to identify and detect surface waves for the purpose of earthquake/explosion discrimination. This is being accomplished through development of high-resolution earth models constrained by inversion of surface wave observations and auxiliary information, which in turn are used to derive surface wave phase and group velocity dispersion curves on a global grid. These dispersion curves are then used to construct phase-matched filters to improve surface wave detection. The availability of high-resolution group velocity curves also makes it possible to use surface waves to improve event location, as suggested by Yacoub (2000), so we have performed a study to assess under what conditions this technique may be useful. This paper is organized into three parts: improvement of regionalized global earth models and dispersion curves; automatic surface wave identification using phase-matched filtering; and location of events using surface wave observations.

Development of Regionalized Earth and Dispersion Models

The most important information required for improving surface wave detection and measurement is accurate global dispersion maps. Consequently, most of our work has concentrated on the development of three-dimensional velocity models of the earth's crust and upper mantle by tomographic inversion of surface wave dispersion measurements. This work uses an extension of the technique described by Stevens and McLaughlin (2001), in which a global earth model with 149 distinct model types on a five-degree grid was developed. That model is now being used for routine surface wave identification at the International Data Centre (IDC). The technique used at the IDC is to compare predicted group velocity dispersion curves derived from these regionalized models with measured dispersion curves from observed surface waves. As discussed later, phase velocities derived from these earth models can also be used to develop phase-matched filters to improve signal-to-noise ratio and optimize the detection test.

The data used to derive our earth models consist of more than 548,000 measurements of surface wave group and phase velocity dispersion from earthquakes and explosions. These measurements were obtained from various sources and are for frequencies ranging between 0.005 and 0.1667 Hz with the great majority of observations between 0.01 and 0.1 Hz. The data set has been derived from a variety of regional and global studies including the following: global surface wave group velocities from earthquakes derived using PIDC GSETT3 data (Stevens and McLaughlin, 1996), augmented with more recent measurements derived from PIDC data; surface wave phase and group velocity dispersion curves from underground nuclear test sites (Stevens, 1986; Stevens and McLaughlin, 1988), calculated from earth models for 270 paths (test site – station combinations) at 10 frequencies between 0.015 and 0.06 Hz; phase and group velocity measurements for western Asia and Saudi Arabia from Mitchell et al.(1996) for 12 paths at 17 frequencies between 0.012 and 0.14 Hz; the global phase velocity model of Ekstrom et al. (1996) for 9 periods between 35 and 150 seconds calculated for each 5-degree grid block from a spherical harmonic expansion of order l=40; group velocity measurements for Eurasia from Ritzwoller et al.(1996) and Levshin et al.(1996) for 20 frequencies between 0.004 and 0.1 Hz with 500 to 5000 paths per frequency; Antarctic and South American group velocity measurements from the University of Colorado (Vdovin et al., 1999; Ritzwoller et al., 1999); high-frequency Eurasian dispersion measurements from University of Colorado (Levshin and Ritzwoller, pers. comm., 2001), and a large set of dispersion measurements from Saudi Arabia provided by Herrmann and Mokhtar at St. Louis University. We have received a large set of data from LLNL for North Africa and Eurasia (Pasyanos, pers. comm., 2001), but are still reviewing the measurements and have not included it in the inversion results described here.

Development of improved earth models and dispersion curves has proceeded using the following approach:

1. The starting point was the 5-degree IDC 149 model set (Stevens and McLaughlin, 2001), which was based on approximately 90,000 dispersion measurements.
2. New dispersion measurements were added to the data set and the same model set was reinverted with the new data.

3. New model types were added in areas with increased data or where the data misfit indicated that new model types were required and a new inversion was performed with the larger data and model set.
4. A procedure was developed for including shallow structure, particularly sediment thicknesses and ocean depths, on a one degree grid while inverting for a limited set of distinct models, most of which remained on a five-degree grid, in the crust and upper mantle.
5. The locations and boundaries of the underlying model types were redefined, starting with the Crust 2.0 model, so that they follow plate boundaries and other geologic constraints. The inversion technique was also modified to allow small variations in Moho depth and layer thickness to be defined on a one-degree grid for each model type.

So, with our current approach, the inversion is performed for shear velocity structures in approximately 500 distinct crust and upper mantle model types, but the shallow structure, bathymetry, as well as small changes in layer thickness and Moho depth, can vary on a one-degree grid (64,800 distinct models). P wave velocities are constrained via a constant Poisson's ratio of 0.27, and density via Birch's Law. The layers vary in thickness (averaging about 10 km) and reach down to a depth of about 250 km. Below 250 km the Earth model is fixed to match PREM. The top few kilometers of the model (consisting of water, ice and/or sediments) is fixed and matches data from 1-degree bathymetry maps made by averaging Etopo5 5 minute measurements of topography, and Laske and Masters (1997) 1-degree maps of sediments. One advantage of inverting for a fixed set of crust and upper mantle structures is that it reduces the problem to a more manageable size. An earth model consisting of 16200 2-by-2 degree cells and with about 10 layers per cell would have on the order of 10^5 free parameters. Our current model consists of 537 model types that reduce the total number of free parameters to 6494. Other advantages of this type of inversion are that it uses all frequencies (and both phase and group velocity) at once, with different frequencies resolving different length scales; the technique keeps similar structures consistent with each other, avoiding fluctuations in nearby points common in more traditional group velocity inversions; and it allows Moho depths, subcrustal layer thicknesses, and lateral boundaries between geologic regions to be added to the model as fixed *a priori* information. The principal disadvantages are that distinct model types must be chosen carefully and added sparingly if needed, and that there is no smoothness constraint between adjacent structures.

The current model under development consists of 537 model types. There are two main varieties of types, those originating from the Crust 2.0 2x2 degree crustal types (Bassin et al., 2000 and Laske et al. 2001) and those based on ocean ages (Stevens and Adams, 2000). The Crust 2.0 models are an improvement of the Mooney et al. (1998) Crust 5.1 model revised and refined to a 2-degree scale. They may include a layer of ice, water, 1-3 layers of sediments, and 3 crustal layers. Because many of the Crust 2.0 models differ only in shallow structure rather than crustal velocity or thickness, we use a somewhat different set of models. We combine similar model types that vary in shallow structure, since we treat those variations as independent constraints, which has the effect of reducing the number of model types relative to Crust 2.0. However, we also separate models in widely separated regions so that results from a model in North America, for example, do not affect a model of the same type in Eurasia. This increases the number of model types. We also reparameterized the structure of the oceans based on ocean age. Previously ocean structures were based on both age and sedimentary thickness. We formed 17 ocean types based on the Muller et al. (1997) isochron map. There are five types for each of the three major oceans: Pacific, Indian and Atlantic. The five types match the age ranges 0 to 10.9 Ma, 10.9 to 20.1 Ma, 20.1 to 40.1 Ma, 40.1 to 83.5 Ma and 83.5 to 180.0 Ma. The remaining two types are for the Arctic Sea for ages 0 to 40.1 Ma, and 40.1 to 180.0 Ma.

Sedimentary structures, bathymetry and lateral boundaries between different oceanic types are included on a 1-degree level of detail. This parameterization serves as an initial model for a series of 3-D tomographic inversions. Regularization is controlled by two parameters, one for a vertical smoothing condition applied to layers in each model type, and a damping parameter. The tomographic inversion has the form shown in equation 1. S_g is the slowness of the g^{th} one degree cell; m_j is the shear wave velocity of the j^{th} layer where j spans all the adjustable layers of all model types. X_{ig} is the length of i^{th} raypath traveled in the g^{th} cell, ? T_i is the travel time residual for the i^{th} raypath. From this equation we can see that 64800 one-degree cells are needed to calculate the partial derivatives. One-degree cells are necessary here to carry the information about sediments and bathymetry. However, the free parameters, indexed with j, span a coarser scale, that of

the model types. These equations, plus equations for dampening and smoothing, are solved using the LSQR method. 20 send phase and group velocity maps are shown in figures 1 and 2.

$$\sum_j \partial m_j \sum_g \frac{\partial S_g}{\partial m_j} X_{ig} \partial T_i \qquad (1)$$

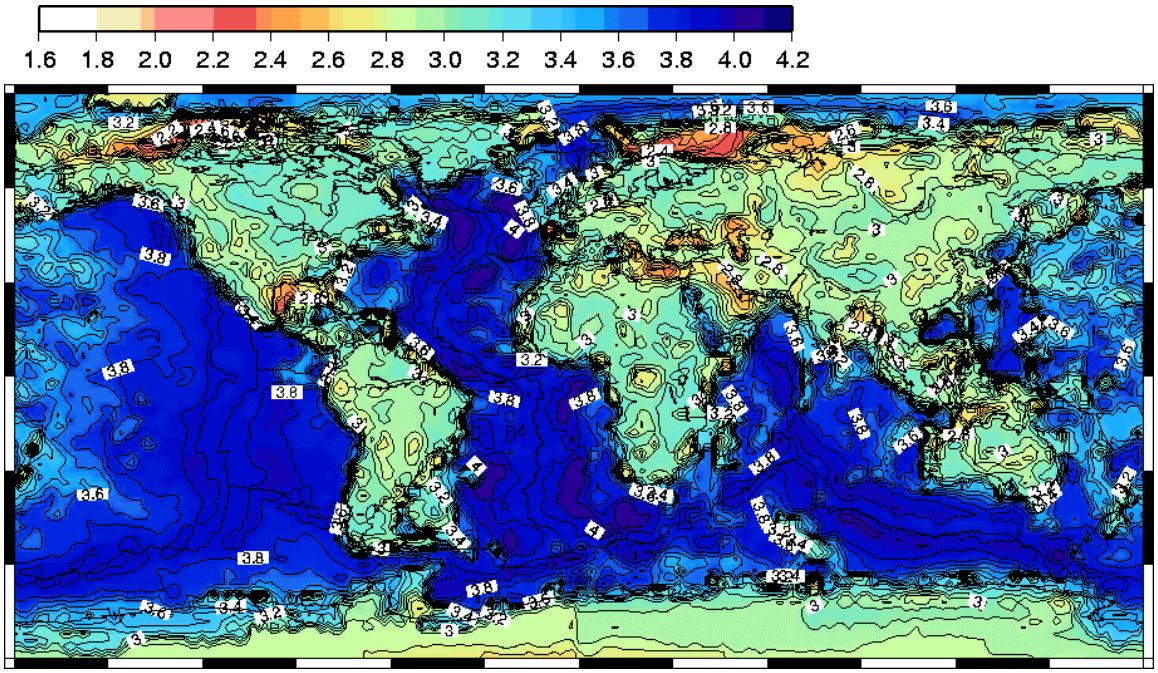

Figure 1. 20-second group velocity map.

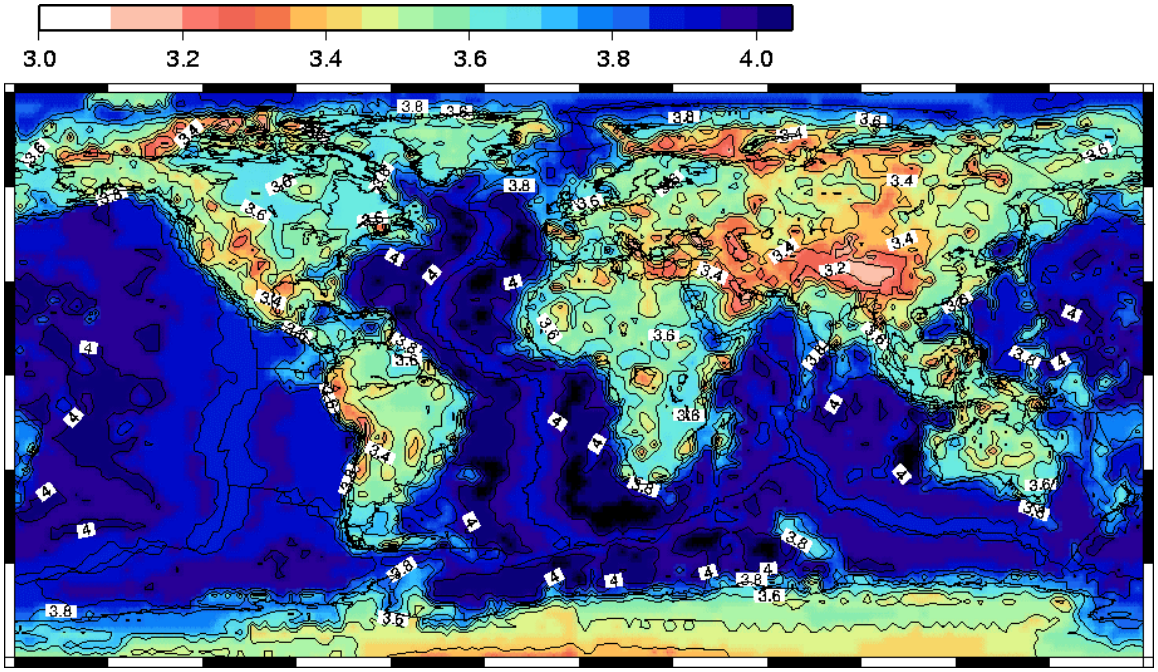

Figure 2. 20-second phase velocity map

The depth profiles of the three main oceanic types are shown in figure 3.

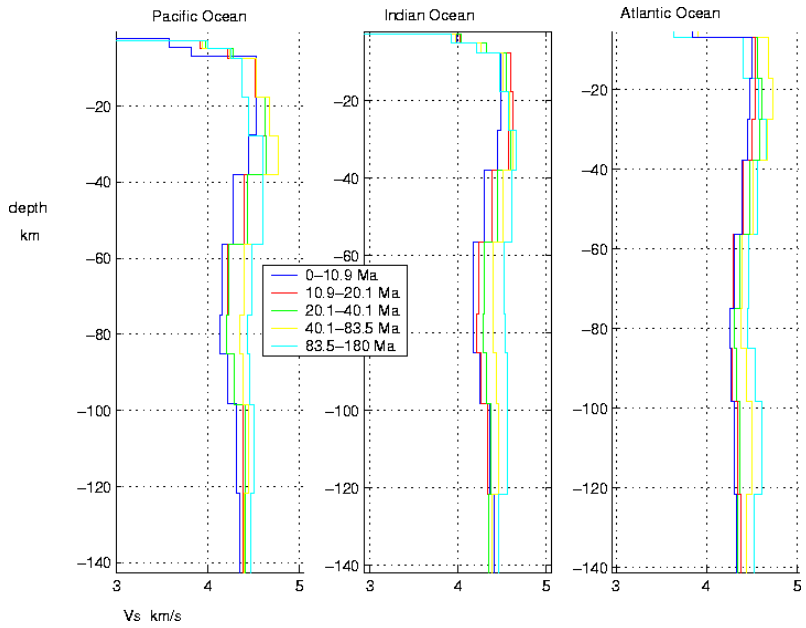

Figure 3. Shear wave velocity depth profiles for the main fifteen ocean types. These results are consistent with thermal models of oceanic lithosphere.

Automatic Surface Wave Detection Using Phase-Matched Filtering

Automatic identification of surface waves at the International Data Centre is currently performed using the processing program Maxsurf by narrow-band filtering the data at several frequencies and then comparing the arrival times with a regionalized dispersion model. An automatic surface wave processing program, Maxpmf, has been developed which is similar to Maxsurf except that it applies phase-matched filtering to seismograms and calculates path-corrected spectral magnitudes in addition to M_s. Maxpmf integrates a regionalized phase velocity model to generate a phase-matched filter that is used to compress the surface wave waveforms. Figure 4 below shows an example of waveform compression after application of phase-matched filters to a data set. Figure 5 shows the recommended way to perform surface wave identification using phase-matched filtering, which is to apply narrow-band filters to the phase-match filtered waveforms and then look for arrival times near zero.

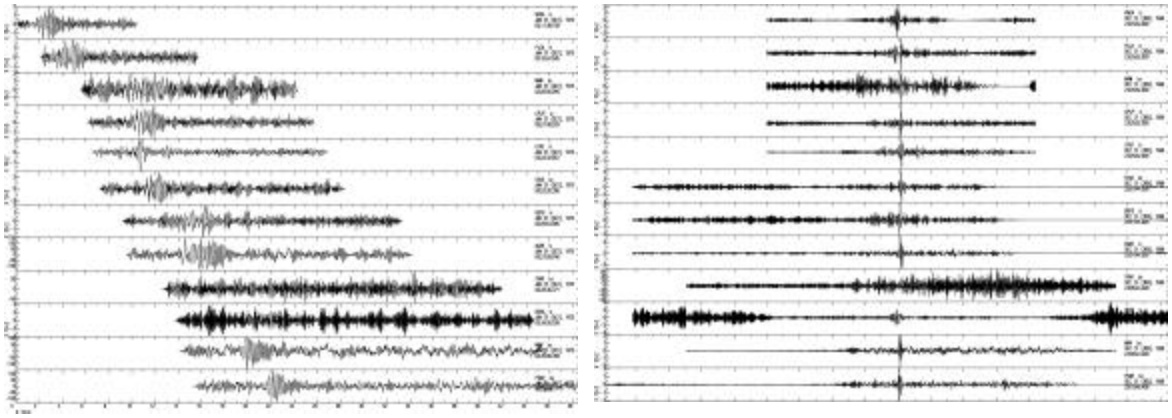

Figure 4. Data in the 5 km/sec to 2 km/sec time window from an m_b 3.9 South Pacific earthquake after transformation to a KS36000 instrument (left) and after compression by phase-matched filtering (right).

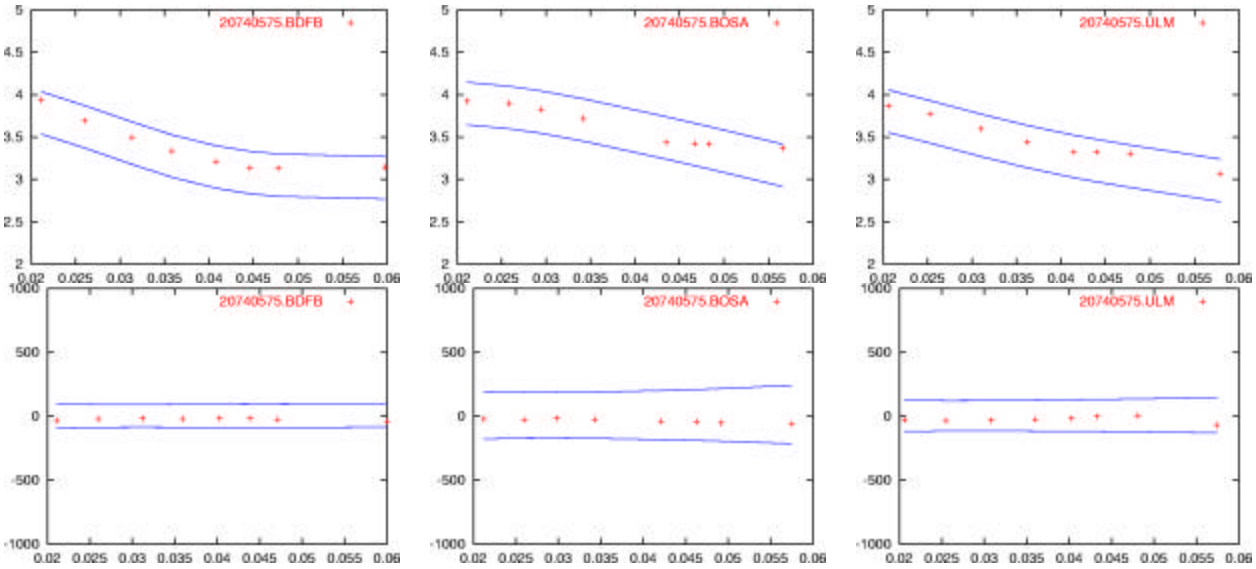

Figure 5. The narrow-band filter detection test (top) compares measured group velocity with a regionalized group velocity model. To improve detection, we phase-match filter the data first, then apply narrow-band filters (bottom). The detection test is applied for the same time interval, but the time is now centered around zero. This example is for an m_b 4.2 South American earthquake observed at BDFB, BOSA, and ULM.

As a test of both the improvement in models and the ability of phase-match filtering to improve detection, we ran Maxpmf on one full day of data and applied both the current narrow-band filtered test and the phase-matched filter test described above to this data set. The results are shown in Figure 6. The four bars show, respectively, the number of detections determined by the current procedure, the number of detections with the best 5-degree model, the number of detections from the current one-degree model, and the number of detections using the one-degree model with phase-matched filtering. Each improved model, and the implementation of phase-matched filtering, shows an improvement. The number of detections increased by 32% over current IDC detections with phase-matched filtering using the most recent one-degree model. The one-degree model used in this test was a modification of the earlier 5-degree model and did not include the modifications discussed earlier to incorporate the Crust 2.0 improvements.

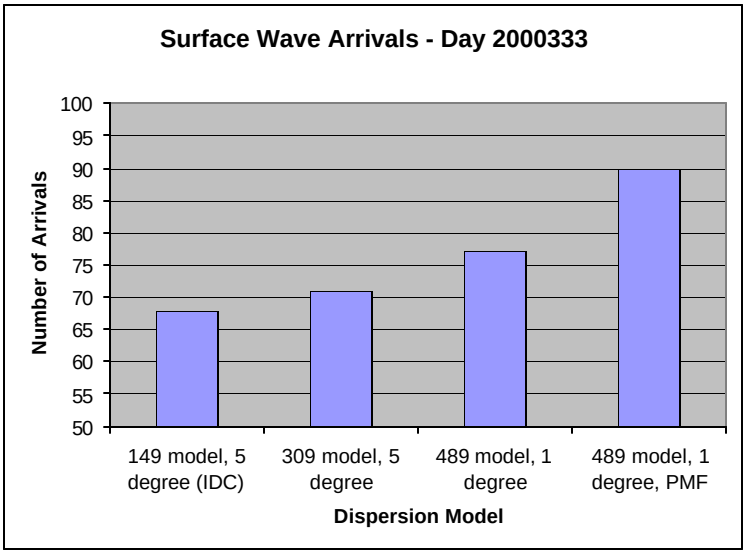

Figure 6. Improvement in the number of detections for a day of data with improvements in the model, and with phase-matched filtering.

As an additional test of the models, we compare observed and predicted dispersion curves for data from nuclear test sites. Tables 1 and 2 show group velocity dispersion residuals and standard deviations in the residuals for periods of 40 seconds and 20 seconds, respectively, for paths from several nuclear test sites. With the expanded data set and 149 models, the results are changed only slightly relative to the inversion with the smaller data set. In fact the results are degraded slightly for the paths from the test sites. This is because the new data caused larger changes in other areas and with the constraint of the small number of models, the data fit became slightly worse in order to allow larger improvements in the areas with concentrations of new data. With 388 models, however, these constraints are relaxed, and the data fit improves for all test sites, and improves quite dramatically for paths in Asia. Curiously, the data fits are not improved with the one-degree model. This result together with the result shown in Figure 8 suggests that the global model is improved, but at the cost of some degradation in paths from the major test sites. We are in the process of investigating the reasons for this now.

Table 1. 40 Second Group Velocity % Average Residuals (Standard Deviations)

Source	IDC 5° 149 Models	5° 149 Models Expanded Data Set	5° 388 Models	1° 489 Models
NTS (59)	0.15 (1.40)	0.22 (1.44)	0.14 (1.20)	-0.17 (1.28)
East Kazakh (40)	0.80 (2.21)	0.85 (2.45)	0.13 (1.11)	0.31 (1.18)
Mururoa (13)	-0.78 (1.43)	-0.73 (1.79)	-0.59 (1.56)	-1.07 (1.48)
Novaya Zemlya (99)	-0.06 (2.06)	0.01 (2.05)	-0.18 (1.81)	-0.10 (1.98)
Amchitka (55)	0.25 (1.39)	0.34 (1.39)	0.35 (1.08)	0.08 (1.18)

Table 2. 20 Second Group Velocity % Average Residuals (Standard Deviations)

Source	IDC 5° 149 Models	5° 149 Models Expanded Data Set	5° 388 Models	1° 489 Models
NTS (58)	-0.47 (2.25)	-0.38 (2.23)	-0.30 (1.88)	-0.08 (2.61)
East Kazakh (40)	-0.75 (1.96)	-0.65 (2.07)	-0.64 (1.44)	-0.05 (1.27)
Mururoa (11)	0.41 (1.43)	0.41 (1.40)	0.53 (1.36)	-0.05 (2.22)
Novaya Zemlya (99)	-0.26 (3.61)	-0.23 (3.66)	-0.43 (3.01)	0.31 (3.28)
Amchitka (54)	0.83 (3.76)	0.70 (3.74)	0.22 (3.23)	0.84 (3.92)

Location Improvement Using Surface Waves

Surface wave arrival times can be used in the same manner as (or together with) P-wave arrival times to determine source location. With a good regionalized group velocity model and well-determined group arrival times, the location could be determined quite accurately, and in cases where P-wave coverage is poor, or azimuthal coverage is limited, using surface wave arrivals has the potential to significantly improve location accuracy. Yacoub (2000) found that he was able to determine the location of 7 Nevada Test Site (NTS) explosions more accurately with surface waves narrow-band filtered at 20 seconds than with P waves. This was done using a constant group velocity of 3.0 km/sec for all paths. This result is attributed to the fact that surface wave group velocities are much slower than P-wave velocities, so that errors in arrival time correspond to significantly smaller errors in distance than the corresponding errors in P wave arrival times, and to the consistency in surface wave arrival times.

We have performed some experiments using our global group velocity models and dispersion measurements to assess the ability to locate events using surface wave arrivals. Table 3 lists location errors from Yacoub (2000) derived using both surface waves and P waves, and the location errors we derived from independent measurements of data at several frequencies from the same events using the regionalized dispersion curves discussed earlier. The results confirm that location estimates are somewhat better than can be obtained from P-wave arrivals at the same stations, although the location errors are somewhat larger than obtained by Yacoub. This may be because Yacoub used a larger and higher quality data set. Also, it should be recognized that Yacoub's P-wave measurements used only data from stations that also had surface wave data, and considerably better results could be obtained from a larger P-wave data set.

Yacoub (2000) found remarkably constant group velocity measurements, all very close to 3.0 km/sec. We cannot confirm this and assume that it must be due either to a particular choice of paths, or some anomaly in the way the measurements were made. Figure 7 shows the distribution of measured group velocities from

all of the explosion data from all test sites. While the mean of the distribution is very close to 3.0 km/sec, there is considerable variation from this value in the data set.

Table 3. Location errors for 3 methods, the number of stations used for each (Yacoub P and surface wave locations used identical sets of stations).

Event	# STA		Location Error (km)		
	Yacoub	IDC	Yac. LR	Yac. P	IDC
Hearts	19	17	11.2	18.3	22.5
Backbeach	19	2	9.7	33.1	NA
Scantling	18	11	25.1	49.9	18.9
Lowball	17	12	16.3	28.3	18.1
Mizzen	14	9	9.8	32.0	34.2
Strake	14	0	13.0	26.0	NA
Sheepshead	12	16	9.2	16.1	13.0
Averages			13 ± 6	29 ± 11	21 ± 7

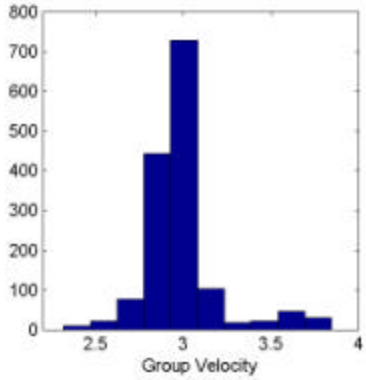

Figure 7. Histogram of measured group velocities of 20-second Rayleigh waves from explosions at all major test sites.

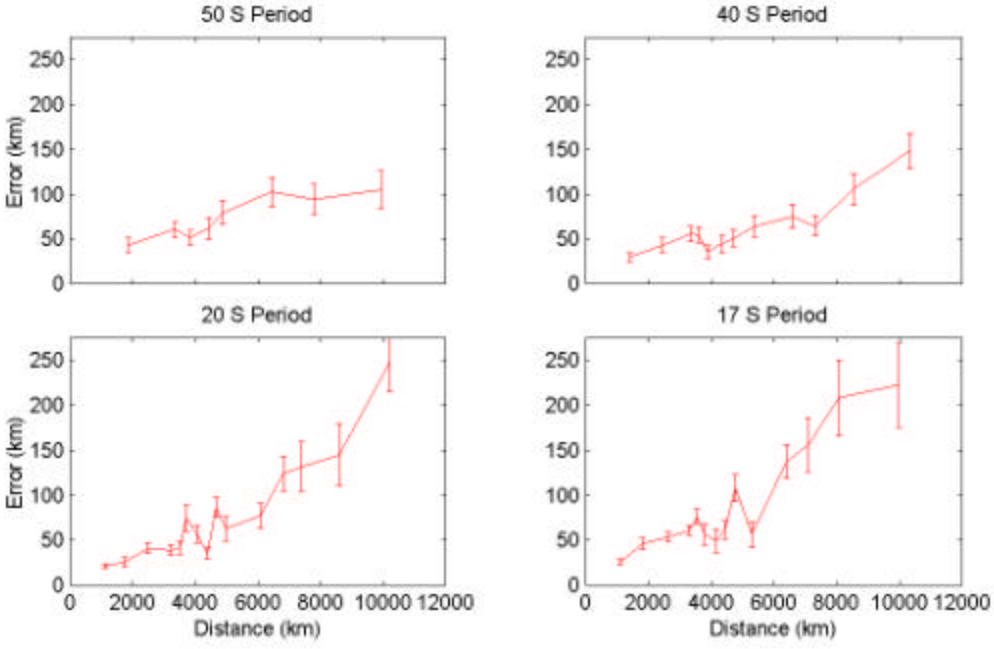

Figure 8. Mean and two standard deviation error bounds of distance estimates from single stations, for different frequencies. There are approximately 100 data per distance bin.

Figure 8 shows the estimated error as a function of distance for single station measurements. In general, the location error increases with distance to the observing station. Lower frequencies, however, degrade much more slowly. However, at shorter distances higher frequency data give more accurate locations.

Figure 9 shows the location error derived from surface wave measurements for the Semipalatinsk test site as a function of the number of recording stations. The results are similar to the NTS results with a typical location error of about 30 km. It is important to note, however, that location accuracy depends as much or more on which stations recorded the event as on how many. Referring to Figure 8, it is clear that surface waves recorded at distances of 3000 km or less provide much better constraints on location than more distant stations. Surface waves are most likely to be useful in constraining location therefore when they are measured at shorter distances and combined with a small number of P-wave measurements. The P-wave measurements on their own may not be very accurate, but even a single surface wave accurately measured at a distance of <2000 km could significantly improve the location.

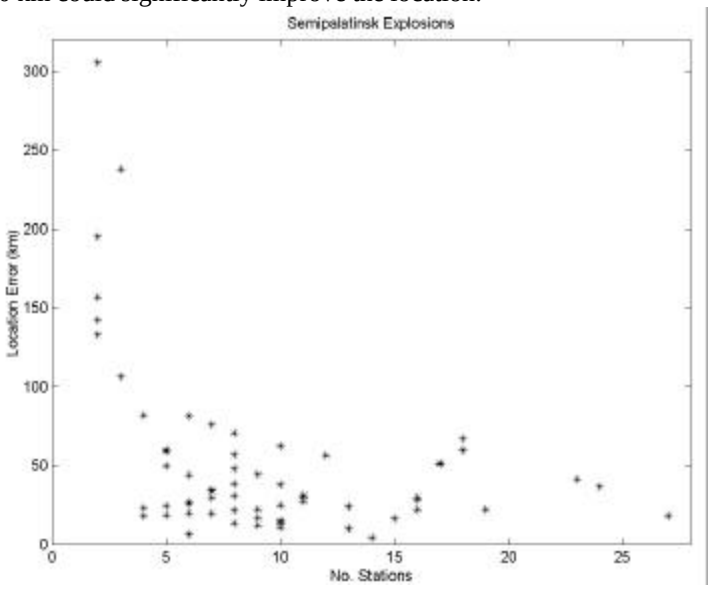

Figure 9. Location errors for Semipalatinsk explosions. The median error for events recorded at 6 or more stations is 30 km.

CONCLUSIONS AND RECOMMENDATIONS

This study has focused on development of improved methods for detection and measurements of surface waves. As part of this effort, we have developed a gradually improving set of global earth models suitable for calculation of phase and group velocity dispersion curves. Over the course of this study, the earth models have evolved from a five-degree model based on 90,000 dispersion measurements to a one-degree model based on over 500,000 measurements. Currently, we are incorporating improvements in boundaries and constraints on shallow structure and Moho depth using the Crust 2.0 models to improve the starting models for the tomographic inversions. We have used phase velocities derived from these models to form phase-matched filters, and developed an improvement on the surface wave detection algorithm that uses phase-matched filtering followed by narrow-band filtering for detection. We performed a test on one day of data at the PIDC with several dispersion models and found a significant improvement using this technique. We have also tested the use of surface waves for location. Although we cannot confirm improvement as significant as suggested by Yacoub (2000), it does appear that surface waves can add an additional constraint that could significantly improve location, particularly in cases where there are only a few P arrivals and the surface waves are measured on short paths.

ACKNOWLEDGEMENTS

We thank M. H. Ritzwoller of Colorado University and M Pasyanos and of Lawrence Livermore National Lab. for providing us with new data.

REFERENCES

Bassin, C., Laske, G. and Masters, G. (2000), The Current Limits of Resolution for Surface Wave Tomography in North America, EOS Trans AGU, 81, F897.

Ekstrom, G., A. M. Dziewonski, G. P. Smith, and W. Su (1996), "Elastic and Inelastic Structure Beneath Eurasia," in *Proceedings of the 18th Annual Seismic Research Symposium on Monitoring a Comprehensive Test Ban Treaty*, Phillips Laboratory Report PL-TR-96-2153.

Laske G. and G. Masters (1997), A Global Digital Map of Sediment Thickness, *EOS Trans. AGU, 78*.

Laske, G., Masters, G. and Reif C., Crust 2.0 (2001), A new global crustal model at 2*2 degrees, http://mahi.ucsd.edu/Gabi/rem.html.

Levshin, A. L., M. H. Ritzwoller, and S. S. Smith (1996), "Group Velocity Variations Across Eurasia," in *Proceedings of the 18th Annual Seismic Research Symposium on Monitoring A Comprehensive Test Ban Treaty,* Phillips Laboratory Report PL-TR-96-2153.

Mitchell, B. J., L. Cong and J. Xie, (1996), "Seismic Attenuation Studies in the Middle East and Southern Asia", St. Louis University Scientific Report No. 1, PL-TR-96-2154, ADA317387.

Mooney, W., G. Laske, and G. Masters (1998), "Crust 5.1: A Global Crustal Model at 5x5 Degrees," *Journal of Geophysical Research*, v. 103, no. B1, pp. 727-747.

Müller, R. D., R. R. Roest, J. Royer, L. M. Gahagan, and J. G. Sclater (1997), "Digital isochrons of the world's ocean floor", *J. Geophys. Res*., 102, 3211-3214.

Ritzwoller, M. H., A. L. Levshin, L. I. Ratnikova, and D. M. Tremblay (1996), "High Resolution Group Velocity Variations Across Central Asia," in *Proceedings of the 18th Annual Seismic Research Symposium On Monitoring A Comprehensive Test Ban Treaty*.

Ritzwoller, M.H., O.Y Vdovin, and A.L. Levshin (1999), "Surface wave dispersion across Antarctica: A first look", *Antarctic J. U.S.*, in press.

Stevens, J. L. (1986), "Estimation of Scalar Moments From Explosion-Generated Surface Waves," *Bull. Seism. Soc. Am.*, v. 76, pp. 123-151.

Stevens, J. L. and D. A. Adams (2000), "Improved surface wave detection and measurement using a global regionalized one degree dispersion model," Transactions Am. Geophys. Union, December.

Stevens, J. L. and K. L. McLaughlin (1996), "Regionalized Maximum Likelihood Surface Wave Analysis," Maxwell Technologies Technical Report PL-TR-96-2273, SSS-DTR-96-15562, September.

Stevens, J. L., and K. L. McLaughlin (1988), "Analysis of surface waves from the Novaya Zemlya, Mururoa, and Amchitka test sites, and maximum likelihood estimation of scalar moments from earthquakes and explosions," S-CUBED technical report SSS-TR-89-9953, September.

Stevens, J. L. and K. L. McLaughlin (2001), "Optimization of surface wave identification and measurement," *Pure and Applied Geophysics*, V. 158, no. 7, in press, July issue.

Vdovin, O. Y., J. A. Rial, M. H. Ritzwoller, and A. L. Levshin (1999), "Group-velocity tomography of South America and the surrounding oceans", *Geophys. J. Int*., 136, 324-330.

Yacoub N. (1996), "Maximum Spectral Energy Arrival Time of Rayleigh Waves for Accurate Epicenter Determination and Location Error Reduction", proceedings *of the 22nd Annual Seismic Research Symposium in New Orleans, LA.*